

# A Spatial–Temporal model for grid impact analysis of plug-in electric vehicles <sup>☆</sup>



Yunfei Mu <sup>a,b</sup>, Jianzhong Wu <sup>a,\*</sup>, Nick Jenkins <sup>a</sup>, Hongjie Jia <sup>b</sup>, Chengshan Wang <sup>b</sup>

<sup>a</sup> Institute of Energy, School of Engineering, Cardiff University, Cardiff CF24 3AA, UK

<sup>b</sup> Key Laboratory of Smart Grid of Ministry of Education, Tianjin University, Tianjin 300072, China

## HIGHLIGHTS

- The Spatial Temporal model (STM) runs based on systematic integration of power system analysis and transportation analysis.
- For the first time Origin–Destination analysis was used to model the spatial and temporal characteristics of EV charging load.
- The STM can provide both average and probabilistic values and can identify the critical network components to upgrade.
- Compared with the previous studies in this area, the STM shows more comprehensive and accurate evaluation results.

## ARTICLE INFO

### Article history:

Received 10 July 2013

Received in revised form 16 September 2013

Accepted 5 October 2013

Available online 26 October 2013

### Keywords:

Electric vehicle (EV)  
Distribution network  
EV charging strategies  
Power system planning  
Spatial–Temporal model  
Origin–Destination matrix

## ABSTRACT

A Spatial–Temporal model (STM) was developed to evaluate the impact of large scale deployment of plug-in electric vehicles (EVs) on urban distribution networks. The STM runs based on the integration of power system analysis and transportation analysis. Origin–Destination (OD) analysis from intelligent transportation research was used to model the EV mobility. Based on the EV technical and market information provided by the EU MERGE project and the output of OD analysis, a Monte Carlo simulation method was developed within the STM to obtain the EV charging load of each load busbar over time. The STM aims to facilitate power system evaluation and planning, and is able to provide both average values and probabilities of nodal bus voltages and branch loadings. The STM is able to identify the critical network components that will require to be upgraded. A high customer density urban network from the United Kingdom Generic Distribution System combined with geographic information was used as a test system. Two EV charging strategies, “dumb” charging and “smart” charging, were simulated and compared under different EV penetration levels (0%, 25% and 50%) to verify the effectiveness of STM.

© 2013 The Authors. Published by Elsevier Ltd. All rights reserved.

## 1. Introduction

The use of plug-in electric vehicles (EVs) has the potential to increase rapidly due to growing concerns over CO<sub>2</sub> emissions and energy security (reliance on imported gas and oil). In order to realize the target of reducing CO<sub>2</sub> emissions from the domestic transport sector by 14% by 2020, the UK Government has supported EV trials with the anticipation that EVs will play a major role in the future transport sector [1,2].

The main features of EVs are as follows: (1) EV charging loads (ECL) are large and vary over time; (2) EVs cause geographically mobile demand rather than stationary load; (3) EVs are charged for relatively long time periods, and their demand may be coincident with the system peak. The introduction and widespread use of EVs could potentially lead to significant impacts on the electricity distribution infrastructure [3,4]. Without proper network evaluation, planning and EV charging management, substation and circuit rebuilding costs could be substantial.

A number of studies have been carried out to evaluate the impacts of EV charging on power systems. Brouwer stated that a large-scale adoption of EVs would have significant impact on national electric power generation and on distribution networks [5]. Rahman et al. investigated the likely impacts that EV charging load will have on distribution systems and concluded that even low penetration levels of EVs can create new peak loads if sufficient attention is not paid to distribute the charging load throughout the off-peak period [6]. A model developed in [7] was used to

<sup>☆</sup> This is an open-access article distributed under the terms of the Creative Commons Attribution License, which permits unrestricted use, distribution, and reproduction in any medium, provided the original author and source are credited.

\* Corresponding author. Address: Room E/2.19, Cardiff School of Engineering, Newport Road, Cardiff CF24 3AA, UK. Tel.: +44 (0)29 2087 0668.

E-mail addresses: [yunfeimu@tju.edu.cn](mailto:yunfeimu@tju.edu.cn) (Y. Mu), [Wuj5@cardiff.ac.uk](mailto:Wuj5@cardiff.ac.uk) (J. Wu), [JenkinsN6@cardiff.ac.uk](mailto:JenkinsN6@cardiff.ac.uk) (N. Jenkins), [hjjia@tju.edu.cn](mailto:hjjia@tju.edu.cn) (H. Jia), [cswang@tju.edu.cn](mailto:cswang@tju.edu.cn) (C. Wang).

determine the optimum EV charging time as a function of the existing load (excluding EVs), ambient temperature and time of day. However, the above studies considered that all EVs start to charge at the same time from a fully discharged state, which will lead to pessimistic conclusions. To address this problem, Qian et al. developed an improved method to model the stochastic nature of the EV charging time and the initial battery state-of-charge (SOC) [8]. Li et al. proposed a method to model the overall EV charging demand for Probabilistic Power Flow calculations, considering key factors that determine the EV charging behavior [9]. Lojowska developed a joint distribution function by using a copula function to consider the stochastic and correlated natures of EV transportation variables [10]. The charging load drawn by an EV depends on the battery type, battery capacity, and maximum travel range. As a mobile energy demand used by people, the EV charging load is influenced by human daily mobility that determines the EV travel distance within a day (which will determine the battery SOC), EV charging locations, and the time charging starts. From the perspective of distribution network analysis and planning, it is critical to determine the spatial and temporal distribution of EV charging load across the system. Bae et al. proposed a spatial and temporal model of EV charging load for rapid charging station located near a highway exit [11]. Soares utilized a discrete-state/time MARKOV Chain to simulate the EVs mobility [12]. The research in [13] and [14] simulated the EV driving patterns according to the data from national driving patterns and demographics. However, these studies did not consider the fundamental principles of transportation systems, therefore are difficult to accurately reproduce realistic EV traffic flow spatially and temporally, which may cause unrealistic results for grid impact analysis.

Transport research has been greatly facilitated by the rapid development of intelligent transportation systems (ITS), geographic information systems (GIS), global positioning systems (GPS), roadside video/detector systems, and modern communication systems [15–18]. Historic and real-time traffic information, such as the information recorded in an Origin–Destination (OD) matrix, is becoming increasingly available from these new systems, which facilitates the application of OD analysis for analyzing traffic flow characteristics, especially in urban areas. Based on the OD analysis from intelligent transportation research [19–21], a Spatial–Temporal model (STM) was developed to model EV mobility both spatially and temporally. The STM, for the first time, runs based on systematic integration of power system analysis and transportation analysis. Based on the EV technical and market information provided by the EU MERGE project (presented as an EV database) [22] and output of the OD analysis, a Monte Carlo simulation method was developed within the STM to obtain the EV charging load of each load busbar at different time. A high customer density urban network from the United Kingdom Generic Distribution System (UKGDS) combined with its geographic information was used as a test system [23]. Two EV charging strategies, “dumb” charging and “smart” charging, were simulated and compared under different EV penetrations to verify the effectiveness of STM.

## 2. Framework of the Spatial–Temporal model

The framework of the STM is shown in Fig. 1. The MERGE EV database provides the characteristics of battery type, capacity and the maximum travel range of EVs intended for the European market [22]. Based on the information in the database, probability density functions were identified to describe the diversity of EV technologies. OD analysis was used to model the EV mobility, i.e., to obtain the travel distance of each EV within a day and the time/location that charging starts. Hourly OD matrixes were used

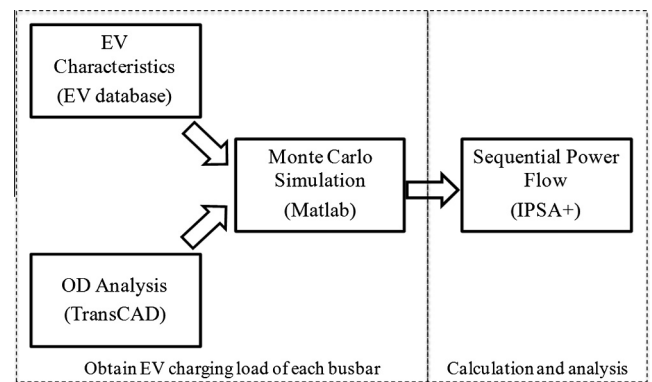


Fig. 1. Framework of the STM.

to define the EV movements over a day. The information supplied by the EV characteristics and OD analysis were used by a Monte Carlo simulation (MCS) to estimate the EV charging load of each busbar at different time throughout a day. Sequential power flow was used to evaluate the impacts of EV charging on power networks. TransCAD, which provided the hourly OD matrixes, along with Matlab and IPSA+ were used to implement the STM [24,25].

## 3. Formulation of the STM

### 3.1. EV Characteristics

#### 3.1.1. EV Classification

Individual EVs were classified based on the following two parallel EV classifications and both were used by the STM.

- *Classification based on the use of transport.* In the UK, 61% of vehicles are privately owned primarily for commuting between home and the working place (Home Based Work, HBW); 9% are company owned and used primarily for business purposes (Non Home Based, NHB), and 30% are owned by those retired from work or who are unemployed (Home Based Other, HBO) [26]. This classification was used to determine the EV travel patterns.
- *Classification based on the type of vehicles.* Based on a survey of the European EV market, four types of EVs were identified in the EV database [22].
  - L7e:** Quadricycle-four wheels, with a maximum unladen mass of 400 kg or 550 kg for goods carrying vehicles.
  - M1:** Passenger vehicle, four wheels up to 8 seats in addition to the driver's seat.
  - N1:** Goods-carrying vehicle, four wheels, with a maximum laden mass of 3500 kg.
  - N2:** Goods-carrying vehicle, four wheels, with a maximum laden mass between 3500 kg and 12,000 kg.

This classification was used to obtain the key parameters (battery type, capacity, maximum travel range, etc.) of an EV battery.

Each EV modeled by the STM was assigned to one of the three purposes of usage (HBW, HBO and NHB) and one of the four vehicle types (L7e, M1, N1 and N2) in order to determine its travel pattern and key battery parameters for Monte Carlo simulation.

#### 3.1.2. Battery type and capacity

In the STM, lead-acid and Li-ion batteries, which are expected to be the two dominant battery technologies in 2020 [27,28], were used to obtain the EV charging loads and corresponding SOC pro-

**Table 1**  
Pdf of EV battery capacity in simulation.

EV group	L7e	M1	N1	N2
Distribution	Gamma	Gamma	Normal	Normal
Parameter	$\alpha = 10.8,$ $\beta = 0.8$	$\alpha = 4.5,$ $\beta = 6.3$	$\mu = 23.0,$ $\sigma = 9.5$	$\mu = 85.3,$ $\sigma = 28.1$
Max (kW h)	15.0	72.0	40.0	120.0
Min (kW h)	5.0	10.0	9.6	51.2

files. It was assumed that 60% of the EV batteries are Li-ion and 40% are lead-acid.

A number of probability distributions were fitted to determine the most suitable probability density function (*pdf*) for the battery capacity ( $Cap_r$ ) of each EV type (L7e, M1, N2, and N2) according to the capacity data from the EV database. The parameters of each *pdf* in Table 1 are defined by (1) for Gamma distribution and (2) for Normal distribution.

$$f(Cap_r; \alpha, \beta) = \frac{1}{\beta^\alpha \Gamma(\alpha)} Cap_r^{\alpha-1} e^{-\frac{Cap_r}{\beta}} \quad (1)$$

$$g(Cap_r; \mu, \sigma) = \frac{1}{\sigma\sqrt{2\pi}} e^{-(Cap_r - \mu)^2 / 2\sigma^2} \quad (2)$$

### 3.1.3. EV maximum travel range

The EV database provides discrete values of the maximum travel range ( $Ran$ ) for different type of EVs. Polynomial fitting was used to determine the mathematical relationship between  $Ran$  and  $Cap_r$ . Taking M1 as an example, the squares in Fig. 2 show the  $Ran$  of each type of M1 EV versus its  $Cap_r$ , and the stars show the result of polynomial fitting.

## 3.2. Origin destination analysis

OD analysis is a widely-used method in transport planning [19–21]. The information needed by the OD analysis in the STM is the geographic information of the studied area, the EV number, and the OD matrixes modelling the EV mobility. OD matrixes are usually available in local transport departments and are obtained by transport survey or from intelligent transportation systems.

- Geographic information of an urban area

**Functional zones:** An urban area was divided into three types of functional zones: residential zones (R), commercial zones (C), and industrial zones (I).

**EV travel distance between two zones:** In transport planning, a centroid is used to represent the geometric centre (the trip

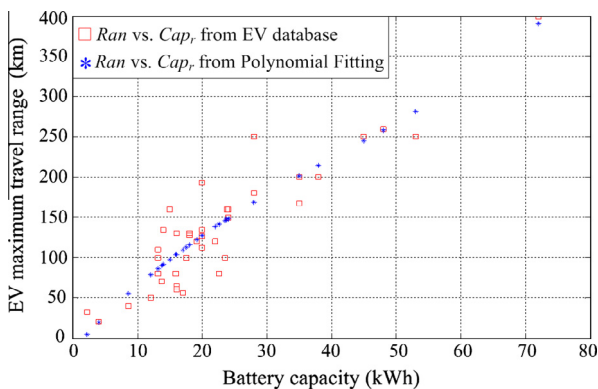


**Fig. 2.** The relationship between battery capacity and maximum travel range.

end) of a functional zone. There are usually several possible routes between the centroids of two zones. In the STM, the travel distance between two zones ( $D_{ij}$ ) was obtained by the normal distribution as described by (3):

$$D_{ij} \sim N(\mu_{ij}, \sigma_{ij}^2) \quad (3)$$

where  $\mu_{ij}$  is the straight line distance between the two centroids of zones  $i$  and  $j$ ;  $\sigma_{ij}$  is the standard deviation for considering the driver's preferences with regard to path selection.

- EV travel time

The daily travel starting time ( $t_s$ ) and finishing time ( $t_f$ ) were determined by the EV classification based on use of the transport (HBW, HBO and NHB).  $t_s$  is the travel starting time of an EV for the first trip of a day;  $t_f$  represents the finishing time of the EV from its last trip of the day. During  $t_s$  and  $t_f$ , an HBW EV has only two trips, while an HBO or NHB EV may have multiple trips. The distributions of  $t_s$  and  $t_f$  for a typical working day (shown in Fig. 3) were obtained from the National Cooperative Highway Research Program [24,29].

- OD matrixes for time of day analysis

In a specific urban area, the daily travel of residents usually follows a regular pattern. In the STM, each EV was assigned with an initial location. OD matrixes were then used to model the EV mobility from setting off to termination for a whole day [19–21].

Twenty-four hourly OD matrixes ( $B_{m \times m}^{(t,t+1)}$ ,  $0 \leq t \leq 23$ ,  $m$  is the total number of functional zones) were used [24].  $B_{m \times m}^{(t,t+1)}$  denotes the EV movement between  $t$  and  $(t+1)$ . The element  $b_{ij}$  ( $1 \leq i \leq m$ ,  $1 \leq j \leq m$ ) in  $B_{m \times m}^{(t,t+1)}$  represents the number of EVs travelling from zone  $i$  to zone  $j$  between time  $t$  and  $(t+1)$ .  $B_{m \times m}^{(t,t+1)}$  was converted to an hourly probability OD matrix ( $C_{m \times m}^{(t,t+1)}$ ,  $0 \leq t \leq 23$ ) through (4).

$$c_{ij} = b_{ij} / \sum_{j=1}^m b_{ij} \quad (1 \leq i \leq m) \quad (4)$$

where  $c_{ij}$  in  $C_{m \times m}^{(t,t+1)}$  means the probability of EV travelling from zone  $i$  to  $j$  between  $t$  and  $(t+1)$ .

### 3.3. EV charging load

The following steps were used to determine the EV charging load.

- Determine  $Cap_r$  of an individual EV battery.

For each EV, a Monte Carlo simulation was used to generate  $Cap_r$  based on the corresponding *pdf* and constraints in Table 1. If the capacity generated was not within the maximum (Max) and minimum (Min) kW h constraints, the process was repeated until the constraints were satisfied.

- Based on  $Cap_r$  generated in step (a), the corresponding  $Ran$  was determined according to the mathematical relationship between  $Cap_r$  and  $Ran$ , as depicted in Fig. 2.
- OD analysis to simulate the EV movements throughout a day.

The travelling time distributions shown in Fig. 3 were used to determine  $t_s$  and  $t_f$ .  $C_{m \times m}^{(t,t+1)}$  was used to trace the real time location ( $L_{(r,t)}$ ,  $r$  denotes location and  $t$  denotes time) of an EV. The travel distance  $D_{(t-1,t)}^{(ij)}$  between zones  $i$  and  $j$  from time  $(t-1)$  to  $t$  was obtained by (3).  $D_{(t-1,t)}^{(ij)}$  is equal to zero when the EV is parked.

- Determine the slow charging start time  $t_{sc}$ .

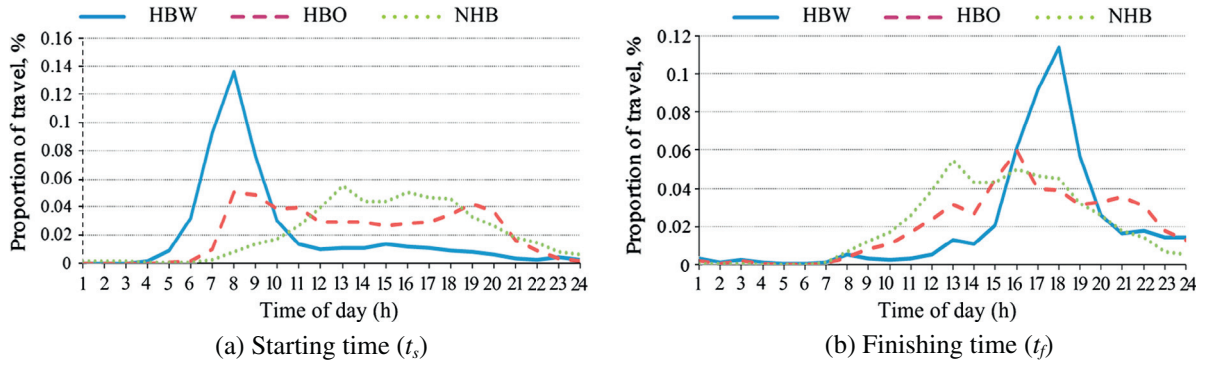


Fig. 3. EV travelling time distributions of HBW, HBO and NHB.

$t_{sc}$  is a key parameter to determine the temporal distribution of the EV charging load. The charging time of an EV battery is determined by people’s daily transport behaviour and the EV charging strategies. Two EV charging strategies were considered to determine  $t_{sc}$ :

– “Dumb” charging

All EVs were assumed to start charging immediately after coming back from their daily trips. Therefore  $t_{sc}$  equals to  $t_f$  that was determined by the distributions shown in Fig. 3.

– “Smart” charging

It was envisaged that there will be an active management system based on two hierarchical control structures, one headed by an Aggregator and other by the system operators (TSO/DSO). Further it was assumed that EV charging is controlled according to the Aggregator’s market negotiations or according to the need of the system operators. Smart charging described by (5) was modelled stochastically with  $\mu$  equal to 1:00 am and  $\sigma$  equal to 5 h considering the real traffic data and real-time electricity rate data in the U.K., which was obtained through optimisation for the minimum charging cost [8]. Compared with the “dumb” charging, “smart” charging can not only realize a shift of EV charging load from the system peak demand time to the valley hours, but also reduce the charging.

$$f(t_{sc}; \mu, \sigma) = \frac{1}{\sqrt{2\pi\sigma^2}} e^{-\frac{(t_{sc}-\mu)^2}{2\sigma^2}} \quad (5)$$

(e) Determine the SOC when an EV starts to charge.

Assuming the SOC drops linearly with the travel distance [8,10], the real time SOC of an EV at time  $t$ ,  $SOC_t$  ( $t \geq t_s$ ), was obtained by tracing the SOC hourly from  $t_s$  and is depicted in (6) and (7):

$$SOC_t = \eta \cdot [SOC_{t-1} - D_{(t-1,t)}^{(ij)} / Ran] \quad t > t_s \quad (6)$$

$$SOC_{t_s} = SOC_0 \quad (7)$$

where  $SOC_0$  is the SOC of an EV before travel and it varies uniformly in the range of [0.8, 0.9] (80–90% SOC was used to maintain the lifetime of a battery [22]); a energy efficiency coefficient  $\eta$  was introduced to consider the energy loss of an EV caused by the acceleration and deceleration processes during the real-world travel (stop-and-go traffic), and it varies uniformly in the range of [0.9, 1.0].

The SOC when an EV starts to charge ( $SOC_c$ ) is defined in (8):

$$SOC_c = SOC_{t_{sc}} \quad (8)$$

where  $t_{sc}$  is the slow charging start time which was obtained in step (d).

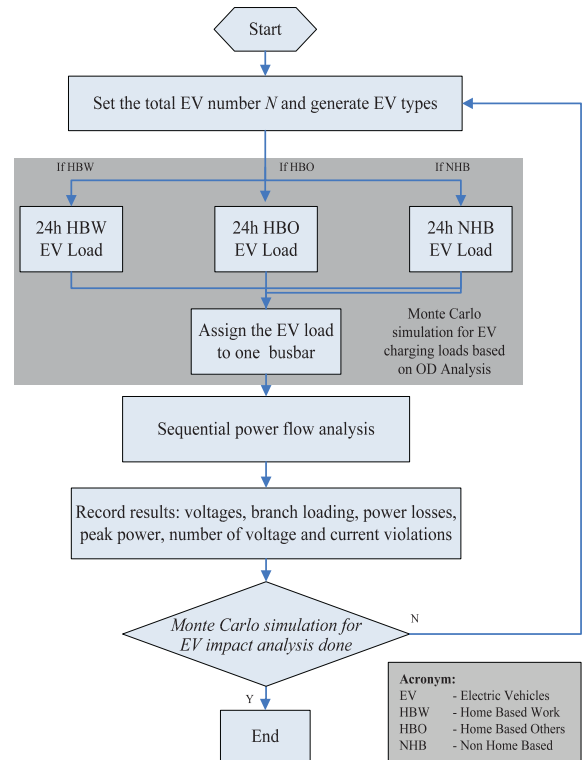


Fig. 4. The overall flowchart of the STM.

(f) Obtain the EV charging load.

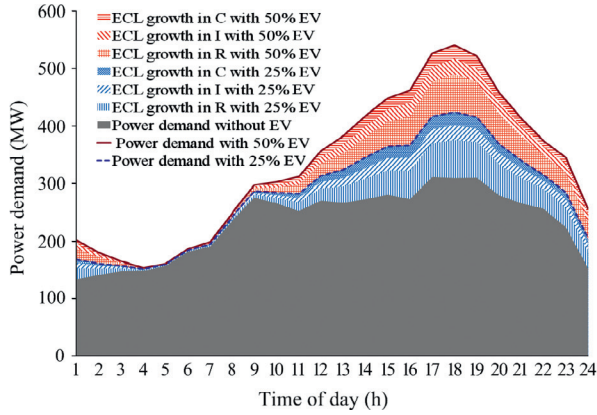
Once  $t_{sc}$  and the corresponding  $L_{(r,t_{sc})}$  were obtained in steps (c) ~ (e) using the Monte Carlo simulation, the power demand at  $L_{(r,t_{sc})}$  was calculated using the method proposed in [30].

For  $n$  EVs, the procedure defined in (a)–(f) was repeated  $n$  times. Each EV charging load at  $L_{(r,t)}$  along a day was recorded. The total EV charging load ( $P_T$ ) for  $m$  ( $m \leq n$ ) EVs charging at  $L_{(r,t)}$  was defined by (9):

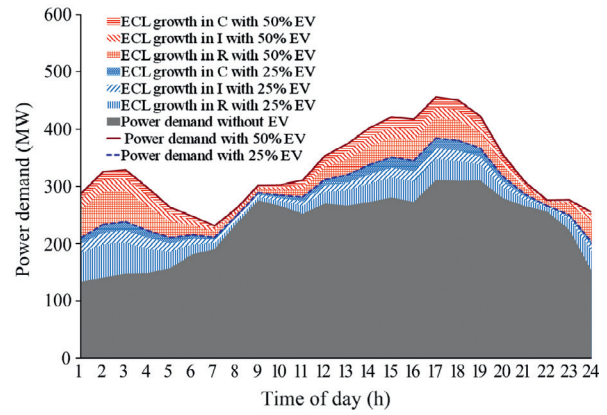
$$P_T = \sum_{i=1}^m P_{t,L_{(r,t)}}^i \quad t = 1, 2, \dots, 24 \quad (9)$$

### 3.4. Sequential power flow

A full fast-decoupled Newton–Raphson power flow model, as shown in Eq. (10), was used in IPSA + to determine the system states (i.e. bus voltage magnitudes and angles) of the electricity network under a given set of steady-state loading and operating condition [31].



(a) Power demand with the “dumb” charging strategy



(b) Power demand with the “smart” charging strategy

Fig. 5. Total power demand of the test network over a typical working day.

$$\begin{cases} \Delta \mathbf{U}^k = -\mathbf{B}^{\prime-1} \Delta \mathbf{Q}(\theta^k, \mathbf{U}^k) \\ \mathbf{U}^{k+1} = \mathbf{U}^k + \Delta \mathbf{U}^k \\ \Delta \theta^k = -\mathbf{B}^{\prime-1} \Delta \mathbf{P}(\theta^k, \mathbf{U}^{k+1}) \\ \theta^{k+1} = \theta^k + \Delta \theta^k \end{cases} \quad (10)$$

$\Delta \mathbf{P}$  and  $\Delta \mathbf{Q}$  are the node active and reactive power unbalance vector, respectively;  $\mathbf{B}'$  is the node susceptance matrix;  $\mathbf{B}^{\prime}$  is the imaginary part of node admittance matrix;  $\theta$  is the vector of bus voltage angle;  $\mathbf{U}$  is the vector of bus voltage magnitude; and  $k$  is the iteration time. Power/current flow and power losses of each branch are then calculated from the system states.

Sequential power flow was implemented by repeating the power flow calculation process depicted in (10) when the steady-state loading or operating condition are updated with a given time interval along with time elapse.

### 3.5. Assumptions in the STM

The following assumptions were made in the STM.

- Monte Carlo simulation was terminated when one of the following two criteria was met:

(1) The maximum number of iterations, or (2) the mismatch of EV charging load between two sequential iterations is small enough as shown in (11):

$$\text{Max} \left| \frac{\sum_{i=1}^{N_{MCS}} L_i}{N_{MCS}} - \frac{\sum_{i=1}^{N_{MCS}-1} L_i}{N_{MCS}-1} \right| < \varepsilon \quad (11)$$

where  $L_i$  is the matrix which stored the 24 h EV charging loads in each zone;  $N_{MCS}$  denotes the number of iteration, and  $\varepsilon$  is the convergence factor.  $\varepsilon$  was set to 0.001 and maximum value of  $N_{MCS}$  was set to 1000.

- Fast charging was conducted when the criteria in (12) or (13) were met and it was assumed that fast charging creates a 15 kW charging load for each EV.

- HBW EVs used fast charging facilities at work places if

$$SOC_r < 0.2 \text{ or } D(SOC_r) < N(D_{wh}, \sigma^2) \quad (12)$$

- HBO and NHB EVs used fast charging during their journey if

$$SOC_r < 0.2 \text{ or } D(SOC_r) < N(D_n, \sigma^2) \quad (13)$$

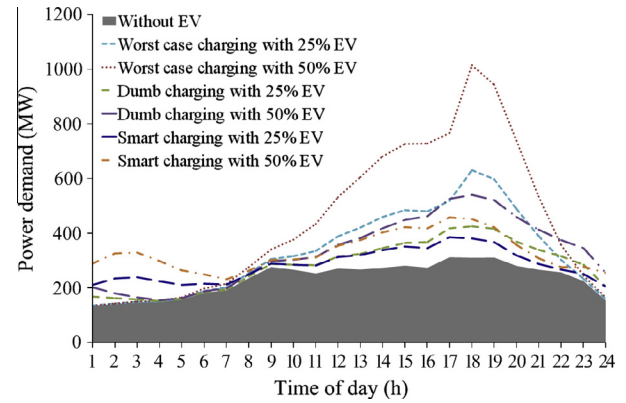


Fig. 6. Comparison of total power demand of the test network from the STM and the worst case scenario.

where  $SOC_r$  is the real-time SOC;  $D_{wh}$  is the straight line distance between the work place and the home;  $D_n$  is the straight line distance between the current place and the next destination;  $D(SOC_r)$  is the distance that can be travelled using the available battery capacity. In order to maintain the lifetime of a battery, the SOC should not drop below 0.2 [22].

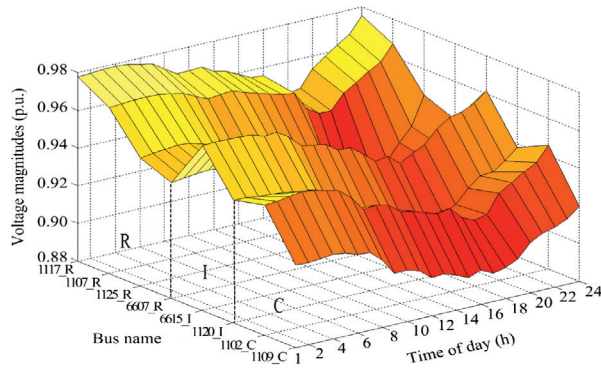
- Each zone  $L_r$  may contain several busbars. It is crucial to obtain EV location in order to allocate its charging load to a specific network busbar once the total EV charging load of  $L_r$  at time  $t$  ( $1 \leq t \leq 24$ ) was determined. The EV charging load at each busbar belonging to  $L_r$  was assigned in proportion to its non EV load at time  $t$ . For instance, if an EV is parked in a residential zone at time  $t$ , the EV charging loads will be assigned to all busbars supplying this zone in proportion to their general residential electric loads (without EV charging loads) at time  $t$ . The same method applies to the EVs parked in commercial and industrial zones.

### 4. Flowchart of the STM

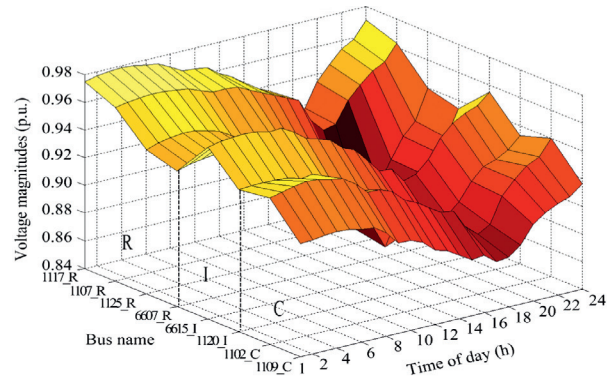
The overall flowchart of the STM is shown in Fig. 4. The flowcharts for different EV groups (HBW, HBO and NHB) to obtain the 24-h EV charging loads are given in the Appendix (Figs. A1–A3).

### 5. Case studies and simulation results

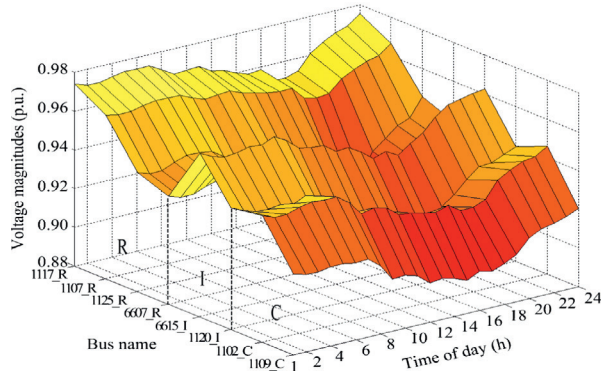
The EHV6 model that represents a typical UK urban underground network [23] was used as the test network. The EHV6



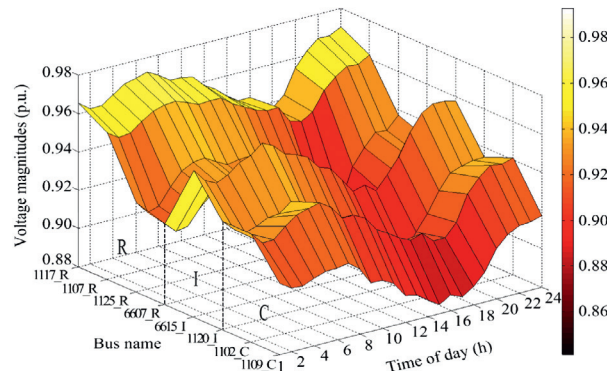
(a) 25% EV penetration with “dumb” charging



(b) 50% EV penetration with “dumb” charging



(c) 25% EV penetration with “smart” charging



(d) 50% EV penetration with “smart” charging

Fig. 7. Nodal voltage magnitudes of bus bars (the subscripts of “\_R”, “\_C” and “\_I” in the busbar names denote the locations in different functional zones).

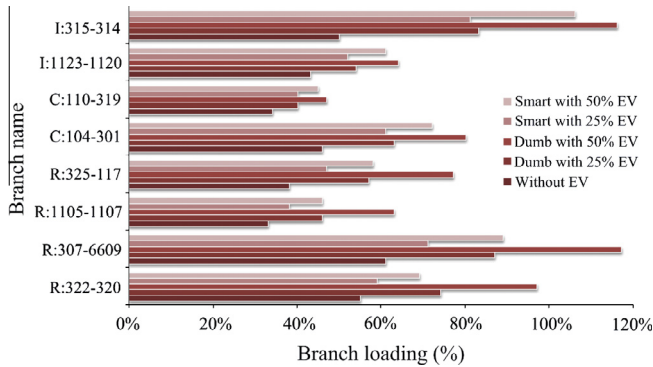


Fig. 8. Branch loadings at the peak load times.

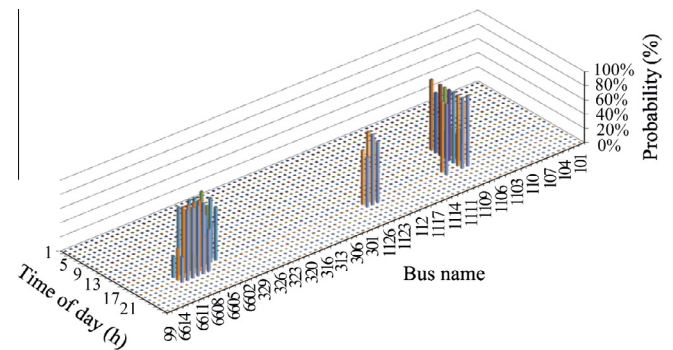


Fig. 10. Low voltage percentage with 50% EV penetration and “dumb” charging.

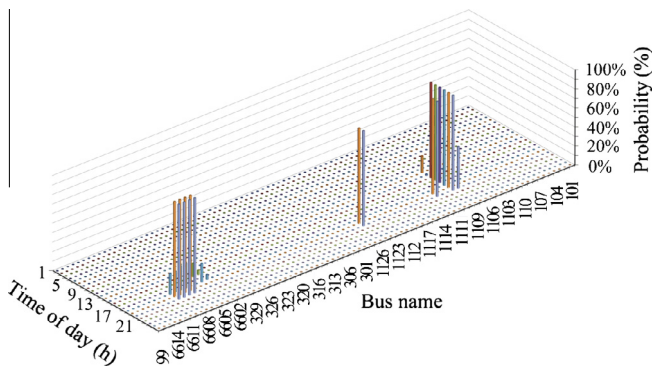


Fig. 9. Low voltage percentage with 25% EV penetration and “dumb” charging.

model combined with its geographic information is shown in Fig. A4 in Appendix. It is composed of three types of functional zones: residential zones (R), commercial zones (C), and industrial zones (I) with different normalized load profiles (without EV charging loads) provided by the UKGDS. These load profiles reflect the characteristics of human activities in each functional zone (R, C, I) [23].

The reference UK peak demand was chosen as 68 GW and the reference total amount of vehicles in the UK was 28.4 million in 2010 [26,32]. The peak demand of the EHV6 test network is 300 MW, which is 0.44% of the reference UK peak demand. The total vehicle number of the test system was also assumed to be 0.44% of the reference total amount of vehicles in the UK (125000 vehicles). Three EV penetration levels were investigated: 0%, 25% and 50% of the vehicles being replaced by EVs. The number of EVs

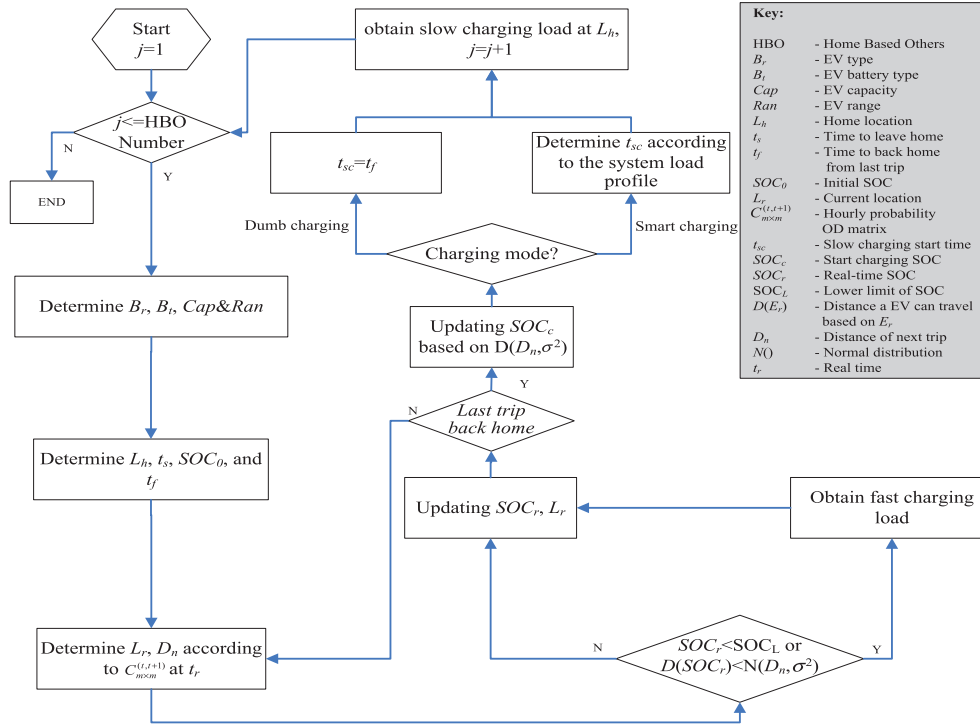


Fig. A1. Flowchart to obtain the HBO EV charging load.

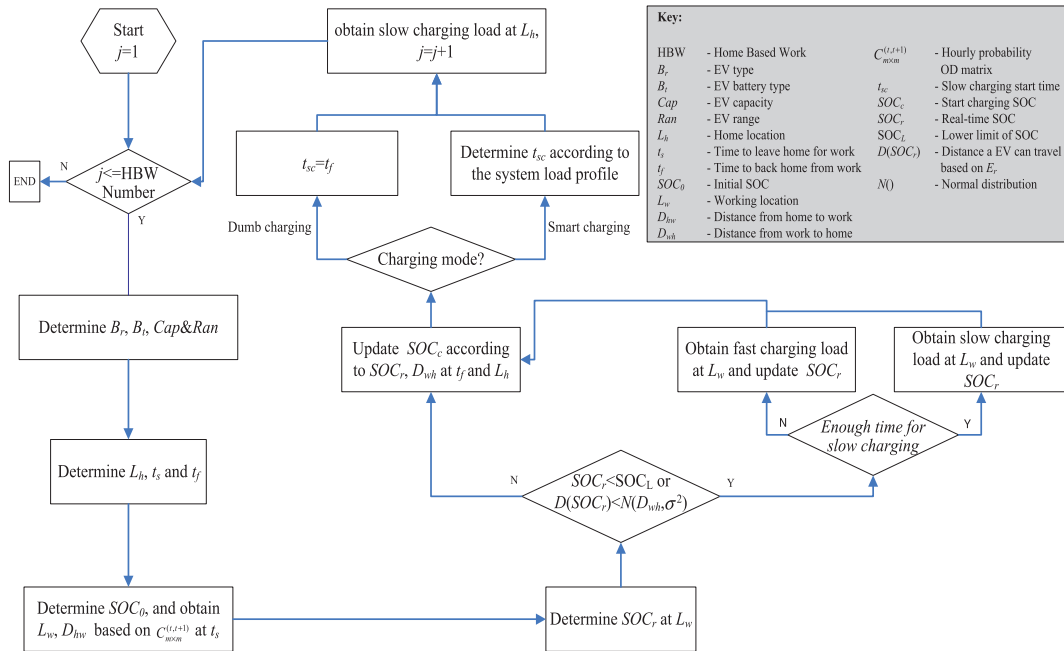


Fig. A2. Flowchart to obtain the HBW EV charging load.

under each EV classification was obtained based on the market information provided by the EV database [22] and is listed in Tables A1 and A2 in Appendix A. The number of EVs in each zone is listed in Tables A3 and A4 in Appendix A.

The hourly OD matrixes was obtained using the function of ‘Time of day analysis’ of TransCAD [24] based on the original-destination through-trip data provided by the National Cooperative Highway Research Program [29].

### 5.1. Power demand

Fig. 5 shows the power demand with the “dumb” and “smart” charging strategies. The different shaded patterns show the proportion of EV charging load in different zones.

As depicted in Fig. 5(a), with “dumb” charging, the peak load was shifted from 17:00 to 18:00 for both EV penetration levels (25% and 50%), and the peak loads were increased by 36% and

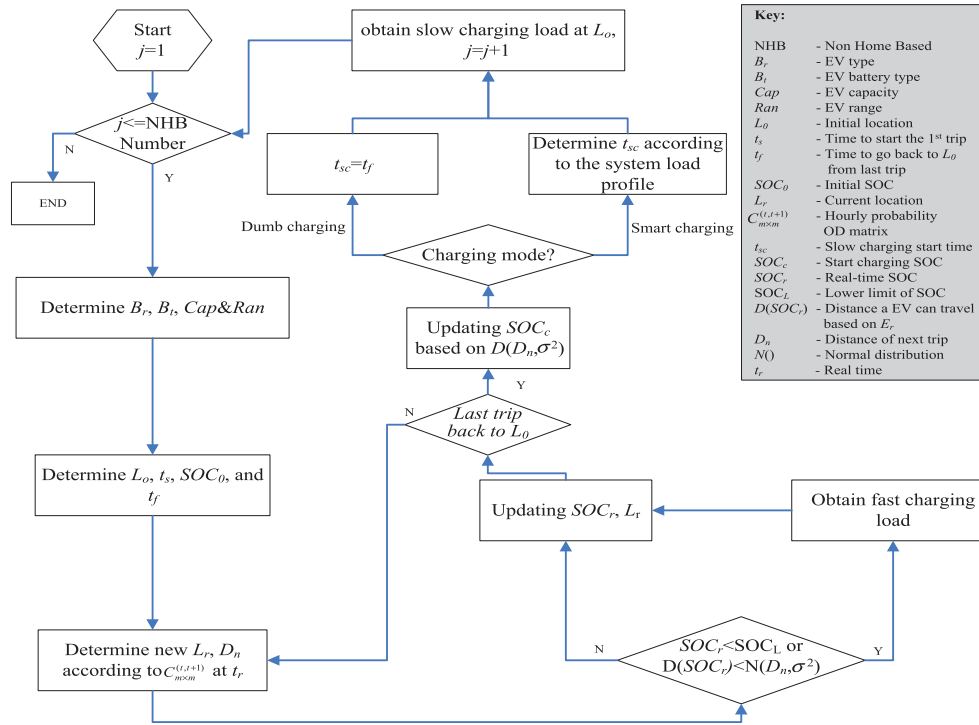


Fig. A3. Flowchart to obtain the NHB EV charging load.

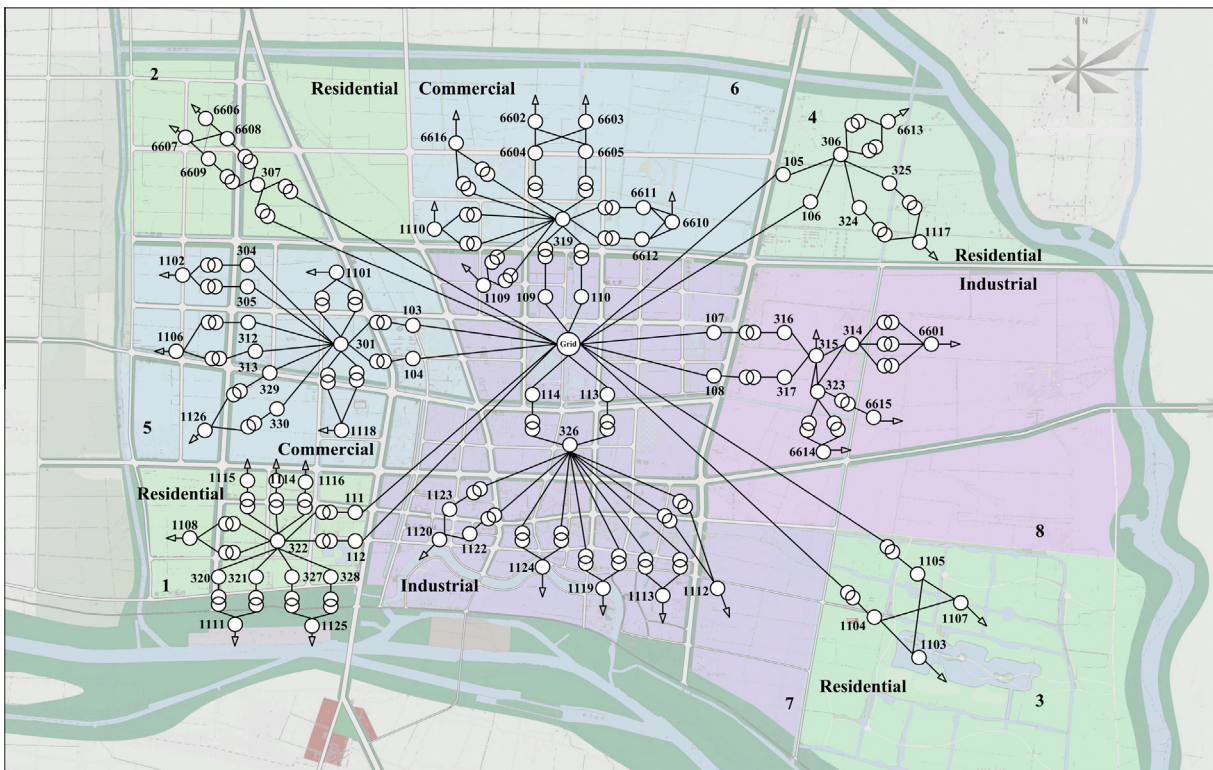


Fig. A4. EHV6 model of the UKGDS with geographic information.

74%, respectively. The daily peak increases were 23% and 47% respectively with “smart” charging (in Fig. 5(b)), which is lower than that with “dumb” charging. Much of the EV charging load

was transferred to fill the “valley” of the original demand curve without EVs. The power demand profiles with “smart” charging are flatter, which means more electricity demand was transferred

to the “off-peak” time reducing the need to upgrade the existing network.

Results of the STM show that the EV charging load had an obvious Spatial–Temporal distribution. The charging load did not grow uniformly in all functional zones. More EV charging loads occurred in the residential zones. Compared with that in the residential zones, the charging load in the commercial and industrial zones showed a more even distribution.

A comparison between results from the STM and the worst case scenario (EVs connected to the network for charging at 18:00 [8]) is shown in Fig. 6. It shows that the worst case scenario provided a much higher demand than that obtained from the STM.

### 5.2. Voltage profiles

The EV charging load has a close correlation with EV mobility, and thus impacts on the nodal voltage both spatially and temporally. The average nodal voltages (summation of the nodal voltage from the Monte Carlo simulations divided by the simulation times) with “dumb” and “smart” charging for one day with hourly time step are presented in Fig. 7. The busbars with the worst voltage profiles in each zone were selected for illustration. As shown in Fig. 7, the voltage magnitudes with “dumb” charging suffered considerable drops between 12:00 noon and at 24:00 midnight, especially in the residential zones at 18:00. The results show that a larger penetration of EVs will cause more severe low voltage in the residential zones than the commercial and industrial zones. The voltage profiles with “smart” charging were improved significantly compared to those with “dumb” charging.

### 5.3. Branch loading

Branch loading is another critical aspect in urban distribution planning, especially with high EV penetrations. Fig. 8 shows the branch loading levels with different EV penetrations and charging strategies under the highest peak load times (as shown in Fig. 5). The branch with the highest loading in each zone was selected for illustration. As expected, the branch loadings increase with the increase of EV penetration. As shown in Fig. 8, with 25% EV penetration, the most problematic branch was 307-6609 in a residential zone with “dumb” charging (87% loading) which is much higher than the value with “smart” charging (71% loading). As the EV penetration increases to 50%, the branch loadings of 307-6609 in a residential zone and 315-314 in an industrial zone increased to 117% and 116%, respectively, with “dumb” charging. Both exceeded their rated capacity. If “smart” charging was used, the branch loading of 307-6609 fell to 89% while that of 315-314 was 106% which is still higher than its rated capacity. The reason was that most EVs in industrial zones belong to the NHB group and these EVs were frequently charged (15 kW charging load for each EV) during the day due to the criteria (12) and (13). Compared with the HBW EVs in residential zones, the control effect from “smart” charging was less obvious.

It can be seen from Fig. 8 that the impact of EV charging load on the branch loading of Zone 8 (e.g. branch 315-314) is much bigger than that of Zone 7 (e.g. branch 1123-1120). This is due to the fact that the NHB EV number in Zone 8 is much bigger than that in Zone 7, as listed in Tables 4 and 5. The branch loading is shown in percentage therefore it also depends on the branch ratings. The ratings of branch 315-314 and 1123-1120 are 17MVA and 13MVA respectively [23].

### 5.4. Probabilistic assessment

Average values are not able to indicate the probability of a specific bus or branch suffering from a problem. The STM is able to

provide probabilities directly. The probabilistic assessment criterion, low voltage percentage (LVP) is given by:

$$LVP = N_{V<0.9} / N \quad (14)$$

where  $N_{V<0.9}$  is the times of bus voltage below 0.9 p.u. during all  $N$  simulations. Figs. 9 and 10 show the probabilistic assessment of nodal voltage under 25% and 50% EV penetration levels with “dumb” charging. It can be seen that some busbars at specific time were vulnerable to low voltages. The results show that the STM can be used as an effective tool to evaluate the impact of EV integration and provide detailed information on the vulnerable sections of the network. It can be used to support decision making of network reinforcement in order to accommodate more EVs.

**Table A1**  
25% Of vehicles replaced by EVs.

EV type	HBW	HBO	NHB	Total amount
M1	11250	8438	6564	26252
N1	0	0	937	937
N2	0	0	937	937
L7e	1250	937	937	3124
Lead-acid	5000	3750	3750	12500
Li-ion	7500	5625	5625	18750
Total no.	12,500	9375	9375	31250

**Table A2**  
50% Of vehicles replaced by EVs.

EV type	HBW	HBO	NHB	Total amount
M1	22500	16876	13128	52504
N1	0	0	1874	1874
N2	0	0	1874	1874
L7e	2500	1874	1874	6248
Lead-acid	10000	7500	7500	25000
Li-ion	15000	11250	11250	37500
Total no.	25000	18750	18750	62500

**Table A3**  
EV number in each zone with 25% of vehicles replaced by EVs.

EV type	HBW	HBO	NHB	Total amount
Zone 1	1531	1148	0	2679
Zone 2	6176	4632	0	10808
Zone 3	2565	1925	0	4490
Zone 4	2228	1670	0	3898
Zone 5	0	0	2677	2677
Zone 6	0	0	2687	2687
Zone 7	0	0	1128	1128
Zone 8	0	0	2883	2883
Total no.	12,500	9375	9375	31250

**Table A4**  
EV number in each zone of with 50% of vehicles replaced by EVs.

EV type	HBW	HBO	NHB	Total amount
Zone 1	3062	2296	0	5358
Zone 2	12353	9264	0	21617
Zone 3	5130	3850	0	8980
Zone 4	4455	3340	0	7795
Zone 5	0	0	5354	5354
Zone 6	0	0	5375	5375
Zone 7	0	0	2255	2255
Zone 8	0	0	5766	5766
Total no.	25,000	18,750	18,750	62,500

## 6. Conclusions

A Spatial–Temporal model was developed to evaluate the impact of large scale deployment of plug-in electric vehicles on urban distribution networks. The STM uses OD analysis to reduce the uncertainties caused by EV mobility. The EV technical and market information provided by the EU MERGE project were analyzed to obtain generalized EV characteristics, e.g. the correlation between battery capacity and the maximum travel range. A Monte Carlo simulation method was developed within the STM to obtain the EV charging load at each busbar at different time. A sequential power flow was used to investigate the grid impact of EVs. A high customer density urban network from the UKGDS was used as the test system. Two EV charging strategies, “dumb” charging and “smart” charging, were simulated under different EV penetration levels (0%, 25%, and 50% vehicles replaced by EVs) to verify the effectiveness of STM.

The STM is able to provide both average values and probabilities of nodal bus voltages and branch loadings. It will facilitate power system planning and evaluation through identifying the most critical network components. The STM is able to provide more realistic results compared to worst case scenario analysis. Compared with the previous studies in this area, the STM uses the OD analysis technique from intelligent transportation research to model the spatial and temporal characteristics of EV charging load for grid impact analysis, which shows more accurate evaluation results.

The OD matrix is more accurate for urban areas with a high population density; therefore the proposed STM is more suitable for the EV impact analysis of urban electricity networks. There are various business cases of EVs, e.g. dispersed charging and the swapping station concept with large centralised charging stations. The STM is an effective tool to analysis the EV impact for the dispersed local charging cases but it also has the potential for the investigation of swapping/charging station location under the swapping station concept.

## Acknowledgements

The authors gratefully acknowledge the RCUK's Energy Programme for the partial financial support of this work through the Top & Tail Transformation Programme Grant, EP/I031707/1 (<http://www.topandtail.org.uk/>) and UK-China EPSRC/NSFC EV Grant EP/L001039/1 and 51361130152. This work was supported in part by the EU FP7 project MERGE.

## Appendix A.

See [Figs. A1–A4](#) and [Tables A1–A4](#).

## References

- [1] Department for Environment Food and Rural Affairs. Local Authority CO<sub>2</sub> Emissions Estimates 2006, Statistical summary; 2008.
- [2] Doucette RT, McCulloch MD. Modeling the prospects of plug-in hybrid electric vehicles to reduce CO<sub>2</sub> emissions. *Appl Energy* 2011;88(7):2315–23.
- [3] Lopes JAP, Soares FJ, Almeida PMR. Integration of electric vehicles in the electric power system. *Proc IEEE* 2011;99(1):168–83.
- [4] Schroeder A. Modeling storage and demand management in power distribution grids. *Appl Energy* 2011;88(12):4700–12.
- [5] Brouwer AS, Kuramochi T, van den Broek M, Faaij A. Fulfilling the electricity demand of electric vehicles in the long term future: an evaluation of centralized and decentralized power supply systems. *Appl Energy* 2013;107:33–51.
- [6] Rahman S, Shrestha GB. An investigation into the impact of electric vehicle load on the electric utility distribution system. *IEEE Trans Power Del* 1993;8(2):591–7.
- [7] Gomez JC, Morcos MM. Impacts of EV battery chargers on the power quality of distribution systems. *IEEE Trans Power Del* 2003;18(3):975–81.
- [8] Qian KJ, Zhou CZ, Allan M, Yuan Y. Modeling of load demand due to EV battery charging in distribution systems. *IEEE Trans Power Syst* 2011;26(2):802–10.
- [9] Li G, Zhang XP. Modeling of plug-in hybrid electric vehicle charging demand in probabilistic power flow calculations. *IEEE Trans Smart Grid* 2012;3(1):492–9.
- [10] Lojowska A, Kurowicka D, Papaefthymiou G, Van der Sluis L. Stochastic modeling of power demand due to EVs using Copula. *IEEE Trans Power Syst* 2012;27(4):1960–8.
- [11] Bae S, Kwasinski A. Spatial and temporal model of electric vehicle charging demand. *IEEE Trans Smart Grid* 2012;3(1):394–403.
- [12] Soares FJ, Lopes JAP, Almeida PMR. A Monte Carlo method to evaluate electric vehicles impacts in distribution networks. In: IEEE Conference on Innovative Technologies for an Efficient and Reliable Electricity Supply (CITRES), Waltham, USA; 2010.
- [13] Kelly JC, MacDonald JS, Keoleian GA. Time-dependent plug-in hybrid electric vehicle charging based on national driving patterns and demographics. *Appl Energy* 2012;94:395–405.
- [14] Saarenpää J, Kolehmainen M, Niska H. Geodemographic analysis and estimation of early plug-in hybrid electric vehicle adoption. *Appl Energy* 2013;107:456–64.
- [15] Zhao Y. Mobile phone location determination and its impact on intelligent transportation systems. *IEEE Trans Intell Transp Syst* 2000;1(1):55–64.
- [16] De Dios Ortuzar J, Willumsen LG. *Modelling transport*, 3rd ed. Hoboken, NJ: Wiley; 2001.
- [17] Sultana A, Kumar A. Optimal siting and size of bioenergy facilities using geographic information system. *Appl Energy* 2012;94(6):192–201.
- [18] Muselli G, Notton G, Poggi P, Louche A. Computer-aided analysis of the integration of renewable-energy systems in remote areas using a geographical-information system. *Appl Energy* 1999;63(3):141–60.
- [19] Hu SR, Wang CM. Vehicle detector deployment strategies for the estimation of network Origin destination demands using partial link traffic counts. *IEEE Trans Intell Transp Syst* 2008;9(2):288–300.
- [20] Seungkirl B, Hyunmyung K, Yongtaek L. Multiple-vehicle origin-destination matrix estimation from traffic counts using genetic algorithm. *J Transp Eng* 2004;130(3):339–47.
- [21] Kudoh Y, Ishitani H, Matsuhashi R, Yoshida Y, Morita K, Katsuki S, et al. Environmental evaluation of introducing electric vehicles using a dynamic traffic flow model. *Appl Energy* 2001;69(2):145–59.
- [22] EU Merge Project. Deliverable 2.1: Modelling Electric Storage devices for electric vehicles, 2010, Task. Rep.; 2010. <[http://www.ev-merge.eu/images/stories/uploads/MERGE\\_WP2\\_D2.1.pdf](http://www.ev-merge.eu/images/stories/uploads/MERGE_WP2_D2.1.pdf)>.
- [23] Foote C, Djapic P, Ault G. Summary of EHV Networks. United Kingdom Generic Distribution Systems (UKGDS); 2006. <<http://monaco.eee.strath.ac.uk/ukgds/>>.
- [24] Caliper Corporation. Caliper TransCAD Version 5.0 GIS User's Guide; Oct, 2007.
- [25] IPSA Power. TNEI Services Ltd. IPSA LFEEngine Version 2.3 Programming Reference Manual; 2010.
- [26] National Statistics, Department for Transport. Transport Statistics Bulletin-Vehicle Licensing Statistics: 2010; April 9, 2011. <<http://www2.dft.gov.uk/pgr/statistics/datatablespublications/vehicles/licensing/latest/vls2010.pdf>>.
- [27] Mendoza A, Argueta J. Performance characterization—GMEV1 Panasonic lead acid battery. Southern California EDISON; Apr. 2000.
- [28] Marid C, Argueta J, Smith J. Performance characterization—1999 Nissan Altra-EV with lithium-ion battery. Southern California EDISON; September 1999.
- [29] William AM, Martin AM. Travel estimation techniques for urban planning. Transport Research Board National Research Council, U.S., NCHRP 365 Rep. B8-29. 6; 1998. <<http://ntl.bts.gov/lib/21000/21500/21563/PB99126724.pdf>>.
- [30] Mu Y, Wu J, Ekanayake J, Jenkins N, Jia H. Primary frequency response from electric vehicles in the Great Britain power system. *IEEE Trans Smart Grid* 2013;4(2):1142–50.
- [31] De Moura AP, De Moura AAF. Newton–Raphson power flow with constant matrices: a comparison with decoupled power flow methods. *Int J Elect Power Energy Syst* 2013;46(1):108–14.
- [32] Metered half-hourly electricity demands; 2010. <<http://www.nationalgrid.com/uk/Electricity/Data/Demand+Data/>>.